

## Two-frequency precession of $\mu^+$ mesons in muonium atoms

I. I. Gurevich and B. A. Nikol'skiĭ

*I. V. Kurchatov Atomic Energy Institute  
Usp. Fiz. Nauk 119, 169-185 (May 1976)*

The review describes experimental and theoretical results on the determination of the frequency  $\omega_0$  of the hyperfine splitting of a muonium atom in a medium. The papers from the I. V. Kurchatov Atomic Energy Institute in which the method of the two-frequency precession of muonium for the determination of the frequency  $\omega_0$  was first proposed are examined in greater detail. The data obtained add in an essential manner to the available information on the interaction of an impurity hydrogenlike atom in condensed media.

PACS numbers: 36.10.Dr, 71.55.-i

### CONTENTS

1. Introduction. . . . .	440
2. Muonium in a Magnetic Field. . . . .	441
3. Two-Frequency Precession of Muonium in a Weak Magnetic Field. . . . .	442
4. Two-Frequency Precession of Muonium in a Strong Magnetic Field. . . . .	442
5. Cessation of Muonium Precession. . . . .	443
6. Experimental Observation of Two-Frequency Precession in a Weak Magnetic Field. . . . .	443
7. Dimensions of an Impurity Muonium Atom in Matter. . . . .	444
8. Two-Frequency Precession of Muonium in Silicon. . . . .	445
9. Calculation of the Magnitude of Hyperfine Splitting of an Impurity Muonium Atom in Germanium and Silicon. . . . .	446
References . . . . .	448

### 1. INTRODUCTION

In recent years a new method is being intensively developed for the study of matter with the aid of  $\mu^+$  mesons. The special feature of a  $\mu^+$  meson consists of the fact that it is a tagged particle, the spin of which can be observed by recording the positrons from the  $\mu^+ - e^+$  decay emitted predominantly in the direction of the  $\mu^+$ -meson spin. Of course the  $\mu^+$  meson disappears in the  $\mu^+ - e^+$  decay, but information remains as to how it was polarized at the instant of decay. Thus, one can study different interactions of  $\mu^+$  mesons with matter in which the  $\mu^+$  meson acts like a light isotope of a proton. On capturing an electron a  $\mu^+$  meson forms a hydrogen-like muonium atom ( $\mu^+e^-$ ). In this review experiments are described on the determination of the frequency  $\omega_0$  of the hyperfine splitting of a muonium atom in matter.

The frequency  $\omega_0$  is determined by observing a phenomenon to which we have given the name of two-frequency precession of a  $\mu^+$  meson in a muonium atom. This phenomenon describes the motion of the spin of a  $\mu^+$  meson in a muonium atom in a magnetic field. Of course, the two-frequency precession does not refer exclusively to muonium. The motion of a nuclear spin will be of the same nature in any other one-electron atom. It is important only that, just as in muonium, the electron should be in an S state, while the nuclear spin should be equal to  $\frac{1}{2}$ . It is also evident that the two-frequency precession is a special case of a more complex, multi-frequency time dependence describing

the motion of nuclear spin in an atom with an arbitrary electronic configuration. As has already been stated above, a muonium atom is distinguished only by the fact that it presents special possibilities for observing the motion of the spin of a nucleus, i. e., of a  $\mu^+$  meson, by the method of recording the positrons from the  $\mu^+ - e^+$  decay.

The two-frequency precession determines the motion of the spin of a  $\mu^+$  meson in a free muonium atom. In practical experiments a muonium atom is obtained by the slowing down of a  $\mu^+$  meson in matter. In the majority of substances the muonium atom, formed there quickly, during a time of  $10^{-11}$  sec, enters into some kind of a diamagnetic compound with compensated electron spins. In this case the spin of the  $\mu^+$  meson can interact only with an external magnetic field, and this leads to Larmor precession with the frequency of a free  $\mu^+$  meson. However, there exist substances in which the impurity muonium atom lives for a sufficiently long time. In such an impurity atom with an uncompensated electron spin the precession of the spin of a  $\mu^+$  meson is similar to the precession in a free muonium atom. Any difference can be due only to the deformation of the electronic wave function for muonium in matter. The deformation of the electronic wave function will alter the magnitude of the interaction of the spins of the  $\mu^+$  meson and of the electron in muonium, and this will lead to a change in the parameters of the two-frequency precession. Observation of the two-frequen-

cy precession of a  $\mu^+$  meson in a muonium atom in matter thus permits one to measure the deformation of its electronic wave function. Below we briefly describe the essence of the phenomenon of two-frequency precession of a  $\mu^+$  meson in muonium.

In a sufficiently weak transverse magnetic field  $B$  a muonium atom in a triplet state precesses as a whole with Larmor frequency  $\omega = eB/2M_e c$ , where  $M_e$  is the electron mass. Observation of the frequency  $\omega$  usually is the experimental proof of the existence of a long-lived impurity muonium atom in a given substance. But such a single-frequency muonium precession is only an approximation which is valid only for relatively short times and weak magnetic fields. In actual fact the precession or the time dependence  $P(t)$  of the direction of the spin of a  $\mu^+$  meson in muonium is determined not by one but by several frequencies. This is a consequence of the fact that the  $S$  state of a muonium atom in a magnetic field represents a four-level system and in the general case is a superposition of four stationary states of energies  $\omega_{ik}$  ( $\hbar = 1$ ) corresponding to different combinations of the spins of the electron and the  $\mu^+$  meson.

The selection rule  $\Delta m = \pm 1$ , where  $m$  is the magnetic quantum number, leads to the fact that of the six possible frequencies  $\omega_{ik} = \omega_i - \omega_k$  ( $i, k = 1-4$ ) only four appear in the expression for  $P(t)$ . The expression for  $P(t)$  is essentially simplified for cases of a weak and a strong external magnetic field  $B$ . The characteristic quantity separating these regions (corresponding in spectroscopy to the Zeeman and the Paschen-Back regions) is the magnetic field  $B_0 = 1594$  Oe. The field  $B_0$  is equal to twice the value of the magnetic field produced by the magnetic moment of the  $\mu^+$  meson at the position of the muonium electron.

The time dependence of  $P(t)$  in weak transverse fields  $B \ll B_0$  is determined, as will be shown below, by two low and two high ( $\sim 10^{10}$  sec $^{-1}$ ) frequencies. If in an experiment the high frequencies are not detected, then after averaging the corresponding terms one obtains the following expression for the observed dependence  $P_{\text{obs}}(t)$  which is the one to which the name of two-frequency muonium precession has been given (cf., (9)):

$$P_{\text{obs}}(t) = \frac{1}{2} \cos \Omega_1 t \cdot \cos \omega t; \quad (1)$$

here  $\Omega_1 = \omega^2/\omega_0$ ,  $\omega_0 = eB_0/M_e c$  is the frequency of the hyperfine splitting of the ground state of muonium. The frequency  $\omega_0$  is determined by the density  $|\psi(0)|^2$  of the electronic wave function at the  $\mu^+$  meson of muonium<sup>[1]</sup>:

$$\omega_0 = \frac{32\pi^2 \mu_e \mu_\mu}{3\hbar} |\psi(0)|^2 = B_0 \cdot 2\mu_e. \quad (2)$$

For vacuum  $\nu = \omega_0/2\pi = 4463$  MHz; here  $\mu_e$  and  $\mu_\mu$  are the magnetic moments of the electron and of the muon.

In strong fields  $B \gg B_0$   $P(t)$  depends practically also on only two frequencies:

$$P(t) \approx \cos \Omega_2 t \cdot \cos \frac{\omega_0}{2} t$$

(cf., (10)) and can also be called two-frequency precession.

From the relations given above it follows that an ex-

perimental observation of the two-frequency precession enables one to determine the frequency of the hyperfine splitting  $\omega_0$ , and, consequently, the value of the electron density at the  $\mu^+$  meson of muonium in a given substance. The quantity obtained  $|\psi(0)|^2$  is of great interest, since muonium in matter behaves like an impurity hydrogen atom, while the experimental determination of the electron density  $|\psi_H(0)|^2$  for hydrogen is not always possible.

The contents of this review are as follows. In Chap. 2 expressions are given for the frequencies  $\omega_{ik}$  and for the function  $P(t)$  which determines the precession of the  $\mu^+$  meson of muonium in a transverse magnetic field. In Chap. 3 the case is considered of a weak magnetic field and it is shown that the precession of the  $\mu^+$  meson of muonium observed in this case is characterized by two frequencies.<sup>[2]</sup> In Chaps. 4 and 5 the two-frequency precession of muonium in a strong magnetic field and the "cessation of precession" are described.<sup>[3]</sup> In Chap. 6 the experimental arrangement is described and values of the frequencies  $\omega_0$  of the muonium atom in different substances determined by the method of the two-frequency precession are given.<sup>[4]</sup> Chapter 7 is devoted to a discussion of the experimental results. Chapter 8 is devoted to the interesting paper<sup>[5]</sup> on the observation of the two-frequency precession of muonium in silicon. In Chap. 9, a study<sup>[6]</sup> is described in which the values of the electron density of muonium  $|\psi(0)|^2$  found experimentally in germanium and silicon are compared with calculated results.

## 2. MUONIUM IN A MAGNETIC FIELD

The time dependence  $P(t)$  of the polarization of the  $\mu^+$  meson of muonium in a transverse magnetic field (precession) is determined, as has been stated in Chap. 1, by four energy eigenvalues  $\omega_i$  of stationary states of muonium in an external magnetic field  $B$ . The expressions for  $\omega_i(B)$  are as follows<sup>[4]</sup>:

$$\left. \begin{aligned} \omega_1 &= \frac{1}{4} \omega_0 + \omega_-, & m &= +1, \\ \omega_2 &= -\frac{1}{4} \omega_0 + \sqrt{\frac{1}{4} \omega_0^2 + \omega_+^2}, & m &= 0, \\ \omega_3 &= \frac{1}{4} \omega_0 - \omega_-, & m &= -1, \\ \omega_4 &= -\frac{1}{4} \omega_0 - \sqrt{\frac{1}{4} \omega_0^2 + \omega_+^2}, & m &= 0, \end{aligned} \right\} I=1, \quad (3)$$

here  $\omega_\pm = \omega(1 \pm \xi)$ ,  $\xi = M_e/M_\mu$ ,  $M_e$  and  $M_\mu$  are the masses of the electron and of the  $\mu^+$  meson. The four values of  $\omega_i$  refer to different values of the spin  $I$  of muonium and of its component  $m$  along the direction of the magnetic field. The functions (3)  $\omega_i(B)$  are shown schematically in Fig. 1. As has been noted in Chap. 1, the precession of the  $\mu^+$  meson in muonium is determined by four frequencies  $\omega_{ik}$  with  $\Delta m = \pm 1$ . These frequencies are

$$\left. \begin{aligned} \omega_{12} &= \frac{\omega_0}{2} + \omega_- - \sqrt{\frac{1}{4} \omega_0^2 + \omega_+^2}, \\ \omega_{23} &= -\frac{\omega_0}{2} + \omega_- + \sqrt{\frac{1}{4} \omega_0^2 + \omega_+^2}, \\ \omega_{41} &= \frac{\omega_0}{2} + \omega_+ + \sqrt{\frac{1}{4} \omega_0^2 + \omega_+^2}, \\ \omega_{34} &= \frac{\omega_0}{2} - \omega_- + \sqrt{\frac{1}{4} \omega_0^2 + \omega_+^2}. \end{aligned} \right\} \quad (4)$$

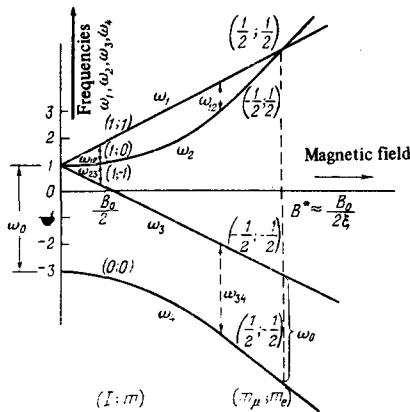


FIG. 1. The energies of stationary states of muonium in a magnetic field. Arrows indicate the frequencies  $\omega_{12}$ ,  $\omega_{23}$  and  $\omega_{14}$ ,  $\omega_{34}$ , which determine the two-frequency precession respectively in weak ( $B \ll B_0$ ) and strong ( $B \gg B_0$ ) fields. In the figure are shown quantum numbers determining the state of the muonium atom in weak and in strong fields: the total magnetic moment  $I$  and its component  $m$  along the direction of the magnetic field for  $B \ll B_0$  and the components of the spins of the  $\mu^+$  meson ( $m_\mu$ ) and of the electron ( $m_e$ ) for  $B \gg B_0$ .

Utilizing the standard computational technique we obtain the following expression for the time dependence  $P(t)$  of the polarization or the precession of the spin of the  $\mu^+$  meson in a transverse magnetic field  $B^{[4]}$ :

$$P(t) = \frac{1}{4} (\cos \omega_{12}t + \cos \omega_{23}t + \cos \omega_{14}t + \cos \omega_{34}t) + \frac{\omega_s}{4\sqrt{(\omega_0^2/4) + \omega_s^2}} (\cos \omega_{12}t - \cos \omega_{23}t - \cos \omega_{14}t + \cos \omega_{34}t). \quad (5)$$

From expression (5) it can be seen that the function  $P(t)$  is of a rather complicated form. Expression (5) is essentially simplified for the cases of a weak ( $B \ll B_0$ ) and a strong ( $B \gg B_0$ ) magnetic field which are investigated respectively in Chaps. 3 and 4. As will be shown, in these cases  $P(t)$  is described by only two frequencies.

### 3. TWO-FREQUENCY PRECESSION OF MUONIUM IN A WEAK MAGNETIC FIELD

In a weak ( $B \ll B_0$ ) magnetic field the frequencies  $\omega_{\pm} \approx \omega = eB/2M_e c$  are much smaller than the frequency  $\omega_0 = eB_0/M_e c$  of hyperfine splitting, as a result of which one can neglect in expression (5) the term in the second bracket and  $P(t)$  turns out to be equal to

$$P(t) \approx \frac{1}{4} (\cos \omega_{12}t + \cos \omega_{23}t + \cos \omega_{14}t + \cos \omega_{34}t), \quad B \ll B_0, \quad (6)$$

while expressions (4) can be rewritten in the form

$$\left. \begin{aligned} \omega_{12} &\approx \omega - \Omega_1, \\ \omega_{23} &\approx \omega + \Omega_1, \\ \omega_{14} &\approx \omega_0 + \omega + \Omega_1, \\ \omega_{34} &\approx \omega_0 - \omega + \Omega_1; \end{aligned} \right\} \quad (7)$$

here

$$\Omega_1 = \frac{\omega_0^2}{\omega} \approx \frac{\omega_0^2}{\omega} = \omega \frac{B}{2B_0} = \frac{1}{4} \omega_0 \left(\frac{B}{B_0}\right)^2 \sim B^2. \quad (8)$$

The expression (6) for  $P(t)$  is simplified if in the experiment (as was the case in our experiment) the high frequencies  $\omega_{14} \approx \omega_{34} \approx \omega_0$  are not detected. In such a case

the rapidly oscillating terms  $\cos \omega_{14}t$  and  $\cos \omega_{34}t$  are averaged and do not contribute to the observed form of  $P_{\text{obs}}(t)$ :

$$P_{\text{obs}}(t) = \frac{1}{4} (\cos \omega_{12}t + \cos \omega_{23}t) = \frac{1}{2} \cos \Omega_1 t \cdot \cos \omega t; \quad (9)$$

here  $\omega = \frac{1}{2}(\omega_{12} + \omega_{23}) = eB/2M_e c$  is the Larmor frequency of precession of muonium in the field  $B$ ,  $\Omega_1 = (\omega_{23} - \omega_{12})/2 \approx \omega^2/\omega_0$  is the beat frequency (cf., (8)). From expression (9) it can be seen that the time dependence of  $P_{\text{obs}}(t)$  is determined by two frequencies and can be named the two-frequency precession or the beats of the spin of the  $\mu^+$  meson of muonium.

Observation of the two-frequency precession enables one to obtain the frequencies  $\omega$  and  $\Omega_1$  and to determine in this manner the frequency  $\omega_0 = \omega^2/\Omega_1$  of the hyperfine splitting of a muonium atom. The experimental determination of the frequencies  $\omega_0$  in different media by the method of two-frequency precession in a weak field is described in Chap. 6.

### 4. TWO-FREQUENCY PRECESSION OF MUONIUM IN A STRONG MAGNETIC FIELD

In Chap. 3 we have considered the precession of a  $\mu^+$  meson in muonium in a weak field. Here we discuss the precession in a strong ( $B \gg B_0$ ) field. In the case  $B \gg B_0$  the factor  $\omega_s/\sqrt{(\omega_0^2/4) + \omega_s^2}$  in expression (5) tends to unity and  $P(t)$  can be written in the form of a two-frequency precession:

$$P(t) \approx \frac{1}{2} (\cos \omega_{12}t + \cos \omega_{34}t) = \cos \frac{\omega_0}{2} t \cdot \cos \Omega_2 t, \quad B \gg B_0; \quad (10)$$

here

$$\Omega_2 = \frac{1}{2}(\omega_{34} - \omega_{12}) \approx 2\xi\omega + \frac{\omega_0^2}{8\omega}, \quad (11)$$

where  $2\xi\omega = \omega_\mu = eB/M_\mu c$  is the frequency of Larmor precession of a  $\mu^+$  meson in the field  $B$ . Thus, in the two-frequency precession (10) the carrier frequency does not depend on the external magnetic field and is equal to  $\omega_0/2$ . The dependence on the field  $B$  of the beat frequency  $\Omega_2$  determines expression (11).  $\Omega_2(B)$  is not monotonic and is shown in Fig. 2. With increasing  $B$  the frequency  $\Omega_2$  at first falls, attaining for

$$\bar{B} = \frac{1-\xi}{1+\xi} \frac{B_0}{2\sqrt{\xi}} \approx \frac{B_0}{2\sqrt{\xi}}$$

its minimum value  $\Omega_2^{\text{min}} = \sqrt{\xi}\omega_0$ , and then begins to in-

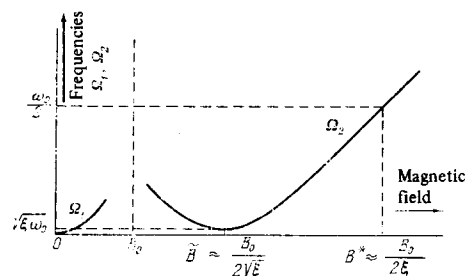


FIG. 2. Dependence on the transverse magnetic field  $B$  of the beat frequencies  $\Omega_1$  and  $\Omega_2$  in expressions (9) and (10) for the two-frequency precession respectively in weak  $B \ll B_0$  and strong  $B \gg B_0$  magnetic fields (arbitrary scale).

crease. Accordingly in fields  $B \ll \bar{B}$   $\Omega_2 \approx \omega_0^2/8\omega \sim 1/B$ , while in fields  $B \gg B_0$   $\Omega_2 \approx 2\xi\omega \sim B$  and attains the value of  $\Omega_2 \approx \omega_0/2$  for

$$B^* = \frac{1-\xi}{2\xi} B_0 \approx \frac{B_0}{2\xi},$$

which corresponds to the intersection of the terms  $\omega_1$  and  $\omega_2$  (cf., Fig. 1). For the vacuum value of  $\omega_0$   $\bar{B} = 11.3$  kOe and  $B^* = 164$  kOe.

A case of a probable observation of the two-frequency precession (10) is described in Chap. 8.

## 5. CESSATION OF MUONIUM PRECESSION

In the region of the Paschen-Back effect when  $\omega \gg \omega_0$  one can observe yet another beautiful effect—the cessation of the precession of the spin of a  $\mu^+$  meson in muonium. The cessation of precession is associated with the crossing of the terms  $\omega_1$  and  $\omega_2$  (cf., Fig. 1) for a field  $B^*$ , when the frequency  $\omega_{12} = 0$ . The crossing of the terms occurs as a result of the fact that the total magnetic moment of muonium in state "1" —  $(\mu_e - \mu_\mu)$  is smaller than in state "2" —  $(\mu_e + \mu_\mu)$ . Therefore the energy of the  $\omega_2$  term grows considerably more rapidly with increasing magnetic field than the energy of the  $\omega_1$  term. From expressions (10) and (11) it follows that as  $B \rightarrow B^*$   $\Omega_2 \rightarrow \omega_0/2$  and  $P(t) \rightarrow \frac{1}{2}(1 + \cos\omega_0 t)$ . In the case of insufficient resolving power of the detecting piece of equipment the term  $\cos\omega_0 t$  is averaged and  $P(t) \rightarrow \frac{1}{2}$ , i. e., cessation of precession is observed. In the case of good resolving power precession with frequency  $\omega_0$  is observed. From expression (10) it follows that slow precession of a  $\mu^+$  meson in fields  $B \rightarrow B^*$  is determined by the frequency  $\omega_{12}$  which in accordance with (4) for  $B \approx B^*$  is approximately equal to

$$\omega_{12} \approx 2\xi \frac{e(B^* - B)}{2M_e c} = \frac{e\Delta B}{M_e c}, \quad (12)$$

where  $\Delta B = B^* - B$ . From (12) it can be seen that for  $B \approx B^*$  the frequency  $\omega_{12}$  is equal to the Larmor frequency of precession of a free  $\mu^+$  meson in the field  $\Delta B$ .

The experimental determination of the field  $B^*$  by the method of cessation of precession can also be utilized for the determination of the frequency  $\omega_0$  of an impurity muonium atom in matter.

## 6. EXPERIMENTAL OBSERVATION OF TWO-FREQUENCY PRECESSION IN A WEAK MAGNETIC FIELD

The scheme of the experimental arrangement for the observation of the two-frequency precession of a  $\mu^+$  meson of muonium in a transverse magnetic field.

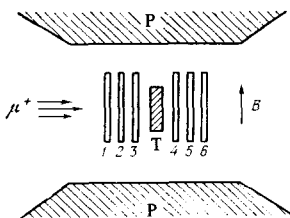


FIG. 3. Schematic outline of the experimental arrangement for the observation of two-frequency precession of the  $\mu^+$  meson of muonium in a transverse magnetic field.

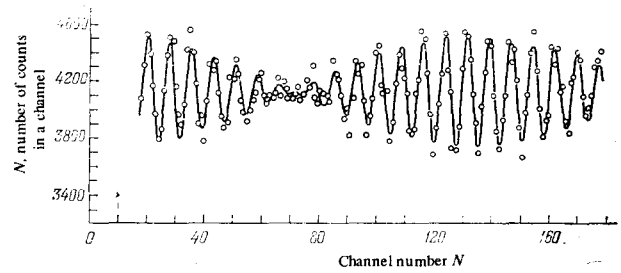


FIG. 4. Two-frequency precession (beats) of the spin of the  $\mu^+$  meson in muonium in fused quartz. The solid curve represents the theoretical dependence  $N(t)$  (13) with parameters chosen by the method of least squares. In the diagram the theoretical and the experimental values of  $N(t)$  have been "corrected" by the decay exponential for the  $\mu^+$  meson  $e^{-t/\tau_0}$  ( $\tau_0 = 2.2 \mu\text{sec}$ ). The channel width of the time analyzer is 1 nsec; the magnetic field is  $B = 95$  Oe. The arrow indicates the channel corresponding to  $t = 0$ .

son in muonium is shown in Fig. 3. A beam of longitudinally polarized  $\mu^+$  mesons from the synchrocyclotron of the JINR was slowed down and stopped in the target M made of the substance under investigation situated in a magnetic field  $B$  perpendicular to the spin of the  $\mu^+$  meson.

The polarization (9)  $P_{\text{obs}}(t)$  of the  $\mu^+$  mesons was measured in terms of the asymmetry of emission of positrons from the  $\mu^+ \rightarrow e^+$  decay in the following manner. The instant  $t_\mu$  of the stopping of a  $\mu^+$  meson in the target M was fixed by a system of signals from the scintillation counters 1 2 3 4 (coincidence of signals from counters 1, 2, 3 and an anticoincidence with counter 4), the instant  $t_e$  of the emission of a positron in the  $\mu^+ \rightarrow e^+$  decay was fixed by the system of signals 4 5 6 3. The time intervals  $t = t_e(4 5 6 3) - t_\mu(1 2 3 4)$  for each case of  $\mu^+ \rightarrow e^+$  decay were analyzed by means of a time-amplitude converter using an amplitude analyzer. The time spectrum  $N(t)$  obtained in this manner for the positrons from the  $\mu^+ \rightarrow e^+$  decay is associated with the change in the polarization (9)  $P_{\text{obs}}(t)$  of  $\mu^+$  mesons with time by means of

$$N(t) = N_0 e^{-t/\tau_0} [1 - c P_{\text{obs}}(t)] \\ = N_0 e^{-t/\tau_0} \left( 1 - \frac{c}{2} e^{-t/\tau} \cos \Omega_1 t \cdot \cos \omega t \right); \quad (13)$$

here  $\tau_0 = 2.2 \times 10^{-6}$  sec is the lifetime of the  $\mu^+$  meson;  $\tau$  is the muonium lifetime;  $c$  is an experimental coefficient for the asymmetry of the angular distribution of the positrons from the  $\mu^+ \rightarrow e^+$  decay, which is determined by the polarization of the  $\mu^+$  mesons in the beam, by the probability of formation of long-lived muonium in the medium, by the solid angle of the positron counter telescope and by the time resolving power of the apparatus.

Experimentally the two-frequency precession (beats) of  $\mu^+$  mesons in muonium is observed in media in which the free muonium atom lives for a sufficiently long time. At the present time it is known that among such media are the noble gases, and also quartz, germanium and ice.<sup>[7]</sup> In Figs. 4 and 5 are shown experimental dependences  $N(t)$  (13) obtained in the course of observing the two-frequency precession in fused quartz and in germanium. The experimental values of the frequen-

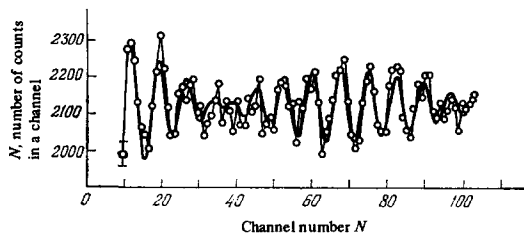


FIG. 5. Two-frequency precession of the spin of the  $\mu^+$  meson in muonium in germanium. Channel width of the time analyzer is 1 nsec; the magnetic field is  $B = 98$  Oe.

cies  $\omega$  and  $\Omega_1$ , and also of  $\tau, N_0$  and  $c$ , appearing in expression (13) were obtained from a comparison by the method of least squares of the theoretical dependence (13) and the experimental spectrum  $N_{\text{exp}}(t)$ . The quantities  $\omega$ ,  $\Omega_1$  and  $\tau$  obtained in this manner for all the investigated substances are shown in Table I. In the same table are also given the parameters of the Pearson relation  $\chi^2$  and their average values  $\bar{\chi}^2$ , equal to the number of experimental points with the number of adjustable parameters subtracted. In the case of quartz beats were observed for different values of the intensity of the magnetic field  $B$ , and this gave us the possibility of experimentally checking the dependence  $\Omega_1 \sim B^2$ , which follows from relation (8). The obtained functional dependence  $\Omega_1(B^2)$  is shown in Fig. 6. From this diagram it can be seen that the experimental values of  $\Omega_1^{\text{exp}}(B^2)$  agree well with theoretical predictions. From the relation  $\Omega_1 \sim B^2$  (cf., also Table I) it follows that the two-frequency precession can be conveniently observed in the case of relatively strong fields  $B$ , when  $\Omega_1$  is sufficiently large. In the case of small fields  $B$ , when  $\omega \gg \Omega_1$ , it is necessary to record many periods of Larmor precession in order to observe one beat period. Such an experiment requires the field  $B$  in the target to be homogeneous with a high degree of accuracy. Therefore in measuring the functional dependence of  $\Omega_1(B)$  in the present experiment the field  $B$  was varied within the limits of  $B = 50-100$  Oe.

## 7. DIMENSIONS OF AN IMPURITY MUONIUM ATOM IN MATTER

The frequencies  $\omega$  and  $\Omega_1$  shown in Table I for different substances enable us to determine the frequencies

TABLE I. Parameters of the two-frequency precession of a  $\mu^+$  meson in ice, germanium and quartz.

$B$ , Oe	$\tau$ , nsec	$\omega$ *, $10^6 \text{ sec}^{-1}$	$\Omega_1$ , $10^6 \text{ sec}^{-1}$	$\nu = \frac{1}{2\pi} \frac{\omega^2}{\Omega_1}$ , MHz	$\chi^2$	$\bar{\chi}^2$
Ice, $T = 77^\circ \text{ K}$						
98	160	858	$24.5 \pm 1.5$	$4791 \pm 300$	285	289
Germanium, $T = 77^\circ \text{ K}$						
98	100	868	$48.1 \pm 1.1$	$2494 \pm 60$	323	290
96	100	848	$42.7 \pm 1.3$	$2682 \pm 80$	330	307
Fused quartz, $T = 300^\circ \text{ K}$						
47	1500	417	$6.1 \pm 0.9$	$4534 \pm 680$	79	57
68	" "	597	$11.6 \pm 0.7$	$4879 \pm 300$	62	67
78	" "	686	$16.8 \pm 0.8$	$4469 \pm 200$	204	186
89	" "	783	$21.3 \pm 0.7$	$4575 \pm 150$	115	69
95	" "	837	$25.7 \pm 0.4$	$4335 \pm 70$	317	305
118	" "	1043	$41.6 \pm 2.0$	$4160 \pm 200$	257	185

\*) The errors in  $\omega$  do not exceed 0.3% and practically do not affect the accuracy of determining  $\nu$ .

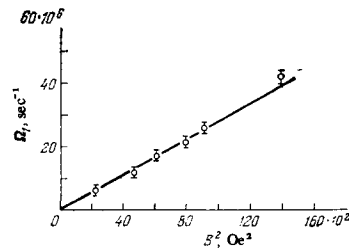


FIG. 6. The experimental dependence of the beat frequency  $\Omega_1$  in quartz on the square of the intensity of the magnetic field  $B$ . The straight line represents the theoretical dependence (8).

$\nu = \omega_0/2\pi$  of the hyperfine splitting of the ground state of the muonium atom in these substances. The values of  $\nu$  obtained in this manner for ice, germanium and quartz are shown in Table I. From Table I it follows that the frequencies  $\nu$  in ice and in fused quartz coincide within the limits of error with the vacuum value  $\nu_{\text{vac}} = 4463$  MHz. For ice  $\nu_{\text{H}_2\text{O}} = 4791 \pm 300$  MHz; for quartz the frequencies  $\nu_{\text{SiO}_2}$  are close for all values of the field  $B$ , the average value is  $\bar{\nu}_{\text{SiO}_2} = 4404 \pm 70$  MHz. The agreement of  $\nu_{\text{H}_2\text{O}}$  and  $\nu_{\text{SiO}_2}$  with the vacuum frequency  $\nu_{\text{vac}}$  indicates that the "dimensions" of muonium in the ground state in ice and in quartz are the same as in vacuum. The frequencies  $\nu_{\text{Ge}}$  (averaged over the two fields  $\bar{\nu}_{\text{Ge}} = 2580 \pm 50$  MHz) in germanium are significantly smaller than the vacuum value  $\nu_{\text{vac}}$ . This means that the Bohr radius of a muonium atom is

$$a = \left( \frac{32\mu_e\mu_H}{3\hbar\omega_0} \right)^{1/3} \sim \left( \frac{1}{\omega_0} \right)^{1/3} \sim \left( \frac{1}{\nu} \right)^{1/3}, \quad (14)$$

while in germanium it is bigger than in vacuum

$$\frac{a_{\text{Ge}}}{a_{\text{vac}}} = \left( \frac{\nu_{\text{vac}}}{\nu_{\text{Ge}}} \right)^{1/3} = 1.20 \pm 0.01. \quad (15)$$

Relations (14) and (15) are naturally valid only on the assumption that the muonium atom in germanium is hydrogenlike. In actual fact the interaction with the medium deforms the wave function of the muonium electron. It is specifically to this that the difference between  $\nu$  in matter and the value of  $\nu_{\text{vac}}$  is related. Therefore, strictly speaking, the frequency  $\nu$  determines only the value of  $|\psi(0)|^2$  of the electron density at the origin (cf. (2)):

$$|\psi(0)|^2 = \frac{3}{10} \frac{\mu}{\mu_e\mu_H} \nu.$$

The values of  $\nu$  for a muonium atom in matter that were obtained above can be compared with the value of  $\nu_{\text{H}}$  for the hyperfine splitting of an impurity hydrogen atom. The values of  $\nu_{\text{H}}$  for fused quartz and ice were measured by the method of electron paramagnetic resonance (EPR) in<sup>[8,9]</sup>. The values of  $\nu_{\text{H}}$  obtained in this manner are given in Table II where the values of  $\nu$  for

TABLE II. Frequencies of the hyperfine splitting of free hydrogen atoms ( $\nu_{\text{H}}$ ) and of muonium ( $\nu$ ) in ice and in quartz in units of  $\nu_{\text{vac}}$ .

Substance	$\nu/\nu_{\text{vac}}$	$\nu_{\text{H}}/(\nu_{\text{H}})_{\text{vac}}$	References
Ice	$1.07 \pm 0.07$	1.00	8
Fused quartz	$0.987 \pm 0.016$	0.985	9

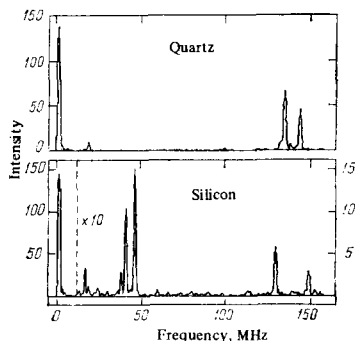


FIG. 7. The frequency spectrum of the precession of a  $\mu^+$  meson of an impurity muonium atom in quartz and in silicon in a transverse magnetic field of  $B = 100$  Oe. The peak of the frequency spectra (from left to right): at the frequency of 1.36 MHz—the precession signal of a free muon; at 19.2 MHz—the signal of the frequency structure of the accelerator beam;  $43.6 \pm 2.9$  MHz—anomalous precession in silicon; two peaks centered at 139 MHz correspond to the usual two-frequency precession of muonium in quartz and in silicon.

a muonium atom in the same substances have also been given for comparison. The value of  $\nu_H$  for ice quoted in Table II was obtained at a temperature of  $4^\circ\text{K}$ . The search by the method of EPR for a free hydrogen atom in ice at a temperature of  $77^\circ\text{K}$  did not give positive results. The coincidence of the frequencies of hyperfine splitting for free atoms of hydrogen and for muonium in matter that follows from Table II shows that the interactions of these atoms with matter are similar and can be studied both by the method of EPR ( $\nu_H$ ), and by the method of two-frequency precession of muonium ( $\nu$ ), complementing one another. One should note this advantage of the two-frequency precession that this method enables one equally effectively to record a free muonium atom both in insulators, where there are no free electrons, and in semiconductors (germanium).

## 8. TWO-FREQUENCY PRECESSION OF MUONIUM IN SILICON

This section is devoted to the work of Brewer, Crow, *et al.*<sup>[5]</sup> on the observation of the two-frequency precession of muonium in silicon. The design of the experiment in this paper is in principle analogous to the one described in Chap. 6. The difference consists only in the interpolation of experimental results which are represented not in the form of the function (9)  $P(t)$  (cf., Figs. 4, 5) but in the form of an expansion of the function  $P(t)$  in a Fourier series. The spectra of the Fourier amplitudes obtained in this manner characterizing the precession of muonium in quartz and in silicon are shown in Fig. 7. From Fig. 7 it can be seen that the precession of muonium in quartz is characterized by two frequencies. The value of  $(\omega_0)_{\text{SiO}_2}$  for quartz determined from these frequencies coincides with the vacuum value of  $\omega_0$  in agreement with the results of<sup>[2,4]</sup>.

In silicon (Si of the  $p$ -type with the number of impurities equal to  $5 \times 10^{12} \text{ cm}^{-3}$ ) at a temperature of  $T = 77^\circ\text{K}$  four frequencies were observed, as can be seen from Fig. 7. Two of them correspond to the two-frequency precession of muonium in a weak magnetic field, which differs from the two-frequency precession

in quartz only by a lower value of  $(\omega_0)_{\text{Si}} = (0.45 \pm 0.02)\omega_0$  and is thus analogous to the two-frequency precession in germanium (cf., Table I). The value of  $(\omega_0)_{\text{Si}}$  obtained above agrees with the result  $(\omega_0)_{\text{Si}} = (0.41 \pm 0.03)\omega_0$  due to Andrianov *et al.*<sup>[10]</sup> obtained from less direct experiments on the measurement of the residual polarization of the  $\mu^+$  mesons in longitudinal magnetic fields. Two other (smaller) frequencies in silicon can be ascribed to the two-frequency precession of muonium produced under some sort of different conditions. But these frequencies exhibit a number of peculiarities and were therefore labeled<sup>[5]</sup> as anomalous. The anomalous frequencies are characterized first of all by the non-monotonic dependence on the intensity of the external magnetic field. This dependence is shown in Fig. 8. From Fig. 8 it follows that the anomalous frequencies can be compared to the frequencies  $\omega_{12}$  and  $\omega_{34}(4)$  in the domain of strong magnetic fields (cf., Fig. 2 which shows the dependence on the magnetic field of the beat frequency  $\Omega_2 = (\omega_{34} - \omega_{12})/2$  in fields  $B \gg B_0$ ). But such a comparison would require renormalization of two parameters at once in expressions (4) for  $\omega_{12}$  and  $\omega_{34}$ : the frequency  $\omega_0$  and the magnetic moment (or the  $g$ -factor) of the electron. Another characteristic feature of the anomalous frequencies consists of the fact that they turn out to depend on the orientation of the single crystal of silicon with respect to the direction of the magnetic field. This dependence is also shown in Fig. 8. The renormalized values of the frequency  $(\omega_0)_{\text{Si}}$  for two different orientations of the silicon crystal turn out to be equal to  $(\omega_0')_{\text{Si}} = (0.0198 \pm 0.0002)\omega_0$  for the case when the [111] crystal axis is parallel to the field and  $(\omega_0'')_{\text{Si}} = (0.0205 \pm 0.0003)\omega_0$  when the [100] axis is parallel to the field. The best value of the  $g$ -factor in both cases is the same:  $g = 13 \pm 3$ . From this it follows that the value of the field  $B_0 = \omega_0/2\mu_e$  (2) for the “anomalous” muonium in silicon is very small:

$$(B_0)_{\text{Si}} = B_0 \left( \frac{\omega_0}{\mu_e} \right)_{\text{Si}} \left( \frac{\mu_e}{\omega_0} \right)_{\text{vac}} = 1594 \cdot \frac{0.02}{6.5} = 5.3 \text{ Oe}.$$

The renormalization of the parameters  $\omega_0$  and  $g$  indicated above naturally represents only a phenomenological description of the experimental data which can

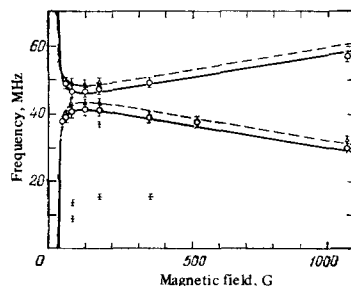


FIG. 8. Dependence of the frequencies of the anomalous precession of muonium in silicon on the intensity of the magnetic field (smooth curves represent the dependence on the field of the frequencies  $\omega_{12}$  and  $\omega_{34}$  with renormalized values of  $\omega_0$  and  $g$ ). The circles and the solid curves correspond to the case when the [111] is parallel to the field, the triangles and the broken curves correspond to the case when the [100] crystal axis is parallel to the field. The horizontal strokes denote individual weak peaks of unknown origin.

correspond to different physical models. One such model is the assumption<sup>[5]</sup> that the anomalous precession corresponds to a surface impurity muonium atom the wave function for the electron of which differs from zero within the limits of several elementary cells. The large size of the surface impurity atom leads to a natural explanation of the small experimental values of the frequency  $(\omega_0)_{Si}$ . In order to explain the strong renormalization of the  $g$ -factor of the muonium electron and the effect of the anisotropy of the interaction of the spin of the  $\mu^+$  meson in a silicon crystal one should abandon the assumption of a contact interaction between the spins of the electron and the  $\mu^+$  meson, since the latter can lead neither to a strong renormalization of  $g$ , nor to any kind of anisotropic effects. Therefore it was assumed that in this case muonium is formed not in its  $1S$  ground state, but in the  $2P$  excited state (observed lifetime of 300 nsec). In the case of a strong spin-orbital interaction a good quantum number is the total angular momentum of the muonium electron  $J$  which in the Breit-Rabi Hamiltonian formally replaces in this case the operator  $S$  for the electron spin. But the total angular momentum  $J$  can be strongly renormalized due to the contribution of the orbital motion, and this determines the strong renormalization of the  $g$ -factor of the electron and the anisotropic effects. Naturally, in such a case the relationship (2) between  $\omega_0$  and  $|\psi(0)|^2$  does not hold, and a measurement of  $\omega_0$  is in this case equivalent to the measurement of the dipole magnetic field produced by the electron at the site of the muonium  $\mu^+$  meson.

The physical model described above introduced to explain the anomalous precession of muonium in silicon is not the only one, although it appears to be the most natural one. In<sup>[5]</sup> other models are also considered, which are based on the interaction of the magnetic moments of the  $\mu^+$  meson and of certain paramagnetic complexes formed as the  $\mu^+$  meson is slowed down in matter.

## 9. CALCULATION OF THE MAGNITUDE OF HYPERFINE SPLITTING OF THE IMPURITY MUONIUM ATOM IN GERMANIUM AND SILICON<sup>[6]</sup>

Above we have described experiments on the determination of the frequency  $\omega_0$  of the hyperfine splitting of an impurity muonium atom in matter. The concept natural in the majority of cases concerning a contact interaction between the spins of the  $\mu^+$  meson and the electron in muonium (an exception is provided by the anomalous precession of muonium in silicon discussed in Chapter 8) means that the measurement of the frequency  $\omega_0$  is equivalent to a measurement of the density  $|\psi(0)|^2$  of the wave function of the muonium electron at the point  $r=0$ , i. e., at the position of the  $\mu^+$  meson. An experimental determination of  $|\psi(0)|^2$  for muonium enables one to check the correctness of the theories in which the properties of an impurity hydrogen atom (or muonium) in matter are calculated. The identity of the properties of hydrogen and of muonium in a solid is illustrated by Table II. It should be emphasized that a measurement of  $|\psi(0)|^2$  for muonium in germanium and in silicon is of particular interest since an impurity atom of hydrogen in these crystals has not been ob-

served to date.

A theoretical estimate of the electron density  $|\psi(0)|^2$  of an impurity muonium atom in germanium and silicon has been carried out in the paper by Wang and Kittel.<sup>[6]</sup> This estimate is not the result of a rigorous calculation of the interaction of muonium in matter, which is very difficult to carry out, but is based on model concepts. An impurity atom of muonium in germanium and in silicon is regarded as a deep donor whose electron moves in the centrally-symmetric field of a  $\mu^+$  meson, while the frequency  $\omega_0$  is determined by the contact interaction between the spins of the electron and the  $\mu^+$  meson. The effect of the medium is taken into account by the introduction of the dielectric constant  $\epsilon$  and by the relatively small renormalization of the electron mass (the mass renormalization can be absent). From this it can be seen that the results of calculations<sup>[6]</sup> can be compared only with the experimental data on the usual two-frequency precession, when the muonium electron is in an  $S$  state. A calculation of the states of the impurity atom corresponding to anomalous precession of muonium in silicon is not given in<sup>[6]</sup>, although the possibility is indicated of the existence in germanium and in silicon of surface donor levels for hydrogen or muonium.

Wang and Kittel present two model calculations: a model involving an empty interstitial vacancy, and a model in which the dielectric constant is determined on the basis of the electron structure of semiconductors.

### A. The model of an empty interstitial vacancy

According to this model the interstitial vacancy in which the impurity muonium atom is situated is of spherical shape of radius  $R$ . At distances  $r < R$  this sphere is empty. The interaction of the muonium electron with the medium manifests itself only for  $r > R$ , i. e., the following functional form of  $\epsilon(r)$  and  $m(r)$  is introduced:

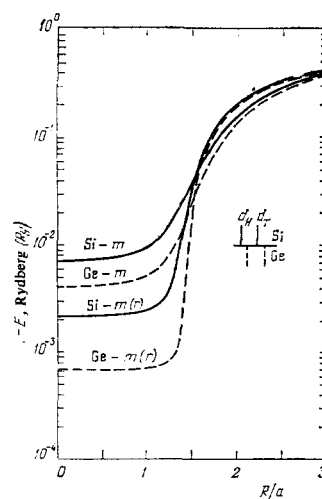


FIG. 9. The ionization energy  $-E$  in vacuum Rydberg units as a function of the radius of the spherical vacancy  $R$  in units of the Bohr radius  $a$ . Calculation according to the empty vacancy model.  $d_H$  and  $d_T$  are the radii of the hexagonal and tetragonal vacancies for silicon and germanium.

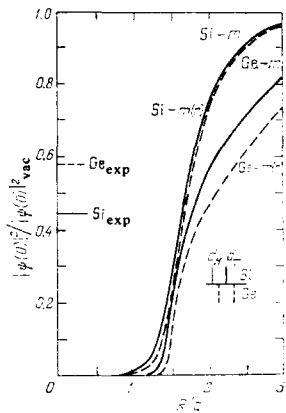


FIG. 10. The density of the wave function of the muonium electron at the site of the  $\mu^+$  meson in units of the vacuum value of this quantity. Calculation according to the empty vacancy model.

$$\epsilon(r) = \begin{cases} 1 & \text{for } r < R, \\ \epsilon_0 & \text{for } r > R, \end{cases} \quad (16)$$

$$m(r) = \begin{cases} m & \text{for } r < R, \\ m^* & \text{for } r > R, \end{cases} \quad (17)$$

here  $\epsilon(r)$  and  $m(r)$  are the permittivity of the medium and the renormalized mass of the muonium electron. In carrying out the calculation the following values of  $\epsilon_0$  and  $m^*$  were adopted:  $\epsilon_0 = 12.0$ ,  $m^*/m = 0.31$  for silicon and  $\epsilon_0 = 15.8$ ,  $m^*/m = 0.17$  for germanium. The relations (16) correspond to the following interaction potential for electrons in muonium:

$$V(r) = \begin{cases} -\frac{e^2}{r} & \text{for } r < R, \\ -\frac{e^2}{\epsilon_0 r} & \text{for } r > R. \end{cases} \quad (18)$$

However, potential (18) does not have the property of continuity. Therefore for the calculations the following potential is utilized

$$V_1(r) = \begin{cases} -\frac{e^2}{r} + e^2 \frac{1 - \epsilon_0^{-1}}{R} & \text{for } r < R, \\ -\frac{e^2}{\epsilon_0 r} & \text{for } r > R, \end{cases} \quad (19)$$

which in its properties is close to  $V(r)$  and which is continuous at the point  $r = R$ .

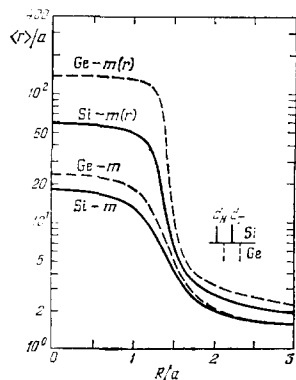


FIG. 11. The average value of the radius of muonium in units of the Bohr radius  $a$ . Calculation according to the empty vacancy model. ( $\text{Si}-m(r)$  for the solid curve on the right).

TABLE III. The density  $|\psi(0)|^2$  of the electron wave function for muonium in germanium and in silicon.

Method of calculation.		$ \psi(0) ^2 /  \psi(0) ^2_{\text{vac}}$	
$m(r)$	$d$	Ge	Si
$m(r) = \begin{cases} m, & r < R \\ m^*, & r > R \end{cases}$	$d_H$	0.506	0.578
	$d_T$	0.565	0.642
$m = \text{const}$	$d_H$	0.787	0.756
	$d_T$	0.860	0.837
Experiment		$0.58 \pm 0.01$	$0.45 \pm 0.02$

The results of the calculations obtained by solving the Schrödinger equation with the interaction potential (19) and taking into account condition (17) are shown in Figs. 9–11. The values of the ionization potential, of the density of the electron wave function for muonium, and of the average radius of the muonium atom shown in those diagrams are plotted as a function of the sphere radius  $R$ . Also in these diagrams are shown the values of the radius of an empty sphere  $d$  in crystals of germanium and silicon. The radius  $d$  was determined from the condition that a sphere of such a radius would fit in an interstitial vacancy on the assumption that the atoms of the lattice represent rigid spheres touching one another. In crystals of germanium and silicon there exist two possible positions of an impurity atom—with hexagonal and tetragonal symmetry of surrounding atoms. In accordance with this one obtains two values of the radius  $d = d_H$  and  $d_T$ , respectively, for hexagonal and tetragonal vacancies. A comparison of the values calculated in this manner with experimental values of the electron density for muonium is given in Table III. From Table III it can be seen that the results of calculation are in sufficiently good agreement with experiment for such a rough model.

The vacancy radius  $d$  for ice calculated by the same method turned out to be larger by approximately a factor four than the Bohr radius for muonium, and this is in agreement with the vacuum value of the frequency  $\omega_0$  for muonium in ice (cf., Tables I and II). An estimate of the radius of a vacancy in the case of fused quartz appears to be difficult.

## B. Determination of the functional form of $\epsilon(r)$ from the electronic structure of germanium and silicon

In accordance with this method of calculation the functional form of  $\epsilon(r)$  for germanium and silicon is

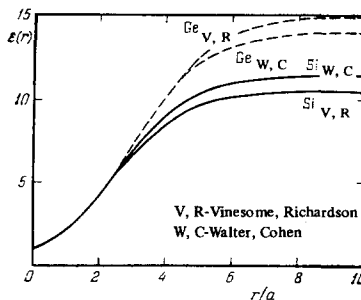


FIG. 12. The functions  $\epsilon(r)$  assumed in calculating the relationship (20).



TABLE IV. Calculated values of the ionization energy  $-E$ , of the density  $|\psi(0)|^2$  of the electron wave function and of the average radius  $\langle r \rangle$  of a muonium atom in Ge and in Si obtained by solving the Schrödinger equation with the potential  $V = -e^2/r\epsilon(r)$ , where  $\epsilon(r)$  is determined by the relationship (20) (here  $\langle r \rangle$  is in units of the Bohr radius  $a$ ).

$\epsilon(r)$	Germanium					Silicon				
	$Q$	$\epsilon_0$	$E, \text{ Ry}$	$ \psi ^2/ \psi _{\text{vac}}^2$	$\langle r \rangle$	$Q$	$\epsilon_0$	$E, \text{ Ry}$	$ \psi ^2/ \psi _{\text{vac}}^2$	$\langle r \rangle$
Walter and Cohen	0.87	14.0	0.116	0.453	2.53	0.92	11.5	0.112	0.427	2.62
Vinsome and Richardson	0.84	14.9	0.128	0.478	2.43	0.92	10.5	0.116	0.429	2.59

assumed to be of the form

$$\frac{1}{\epsilon(r)} = \frac{1}{\epsilon_0} + \left(1 - \frac{1}{\epsilon_0}\right) e^{-Qr}. \quad (20)$$

Such a form of  $\epsilon(r)$  with an appropriate choice of the parameters  $\epsilon_0$  and  $Q$  gives a good description of the functions  $\epsilon(r)$  obtained by Walter and Cohen<sup>[11]</sup> and Vinsome and Richardson<sup>[12]</sup> from the electronic structure of the semiconductors. The functions utilized in the calculation are shown in Fig. 12. The parameters  $\epsilon_0$  and  $Q$  which correspond best to the results of<sup>[11]</sup> and<sup>[12]</sup> are shown in Table IV.

The values of the electron density  $|\psi(0)|^2$  were obtained, just as in the first calculational model, by solving the Schrödinger equation for the muonium electron with the potential  $V = e^2/\epsilon(r)r$ . The results of the calculation shown in Table IV were obtained for a renormalized value of the mass  $m$  of the muonium electron since already in this case the agreement between theory and experiment turns out to be quite satisfactory and the introduction of a renormalization of  $m$  does not improve it.

Good agreement of calculated and experimental values of  $|\psi(0)|^2$  in germanium and in silicon (cf., Tables

III and IV) shows that the concept of an impurity muonium atom situated in an interstitial vacancy is correct. It would be highly desirable to measure also the ionization energy  $E$  of an impurity atom of hydrogen or of muonium. This would enable one to carry out a more detailed comparison of the conclusions of the theory with experiment and, in particular, to determine in which of the two possible vacancies is this impurity atom situated.

- <sup>1</sup>E. Fermi, Z. Phys. 60, 320 (1930); E. Fermi and E. Segre, Z. Phys. 82, 729 (1933).  
<sup>2</sup>I. I. Gurevich, I. G. Ivanter, L. A. Makariyan, E. A. Meleshko, B. A. Nikolsky, V. S. Roganov, V. I. Selivanov, V. P. Smilga, B. V. Sokolov, V. D. Shestakov and I. V. Jakovleva, Phys. Lett. B29, 387 (1969).  
<sup>3</sup>I. I. Gurevich, B. A. Nikol'skii and V. I. Selivanov, Pis'ma Zh. Eksp. Teor. Fiz. 15, 640 (1972) [JETP Lett. 15, 453 (1972)].  
<sup>4</sup>I. I. Gurevich, I. G. Ivanter, E. A. Meleshko, B. A. Nikol'skii, V. S. Roganov, V. I. Selivanov, V. P. Smilga, B. V. Sokolov, and V. D. Shestakov, Zh. Eksp. Teor. Fiz. 60, 471 (1971) [Sov. Phys. JETP 33, 253 (1971)].  
<sup>5</sup>J. H. Brewer, K. M. Crow, F. N. Gyax, R. F. Johnson, B. D. Patterson, D. G. Fleming and A. Schenk, Phys. Rev. Lett. 31, 143 (1973).  
<sup>6</sup>J. Shy-Yih Wang and C. Kittel, Phys. Rev. B7, 713 (1973).  
<sup>7</sup>G. G. Myasishcheva, Yu. V. Obukhov, V. S. Roganov and V. G. Firsov, Zh. Eksp. Teor. Fiz. 53, 451 (1967) [Sov. Phys. JETP 26, 298 (1968)].  
<sup>8</sup>S. Siegel, J. M. Flournoy and L. H. Baum, J. Chem. Phys. 34, 1782 (1961).  
<sup>9</sup>N. N. Bubnov, V. V. Vsevolodskii, L. S. Polak and Yu. D. Tsvetkov, Opt. Spektrosk. 6, 565 (1959).  
<sup>10</sup>D. G. Andrianov, E. V. Minaïshev, G. G. Myasishcheva, Yu. V. Obukhov, V. S. Roganov, G. I. Savel'ev, V. G. Firsov and V. I. Fistul', Zh. Eksp. Teor. Fiz. 58, 1896 (1970) [Sov. Phys. JETP 31, 1019 (1970)].  
<sup>11</sup>J. P. Walter and M. L. Cohen, Phys. Rev. B2, 1821 (1970).  
<sup>12</sup>P. K. W. Vinsome and D. Richardson, J. Phys. C4, 2650 (1971).

Translated by G. Volkoff